A novel stretching and folding characterization method based on geometrical and physiological traits of chaotic and intermittent tracking signals

Fatemeh Babazadeh [a], Mohammad Ali Ahmadi-Pajouh [a,*], Seyed Mohammad Reza Hashemi Golpayegani [a]

[a] *Department of Biomedical Engineering, Amirkabir University of Technology, 424 Hafez Ave., Tehran, P.O. Box 15875-4413, Iran.*

**Corresponding author's Email: pajouh@aut.ac.ir.*

Abstract–The specification of stretching and folding properties, particularly in time series, is of substantial interest. This study is sought to perceive the relationship between stretching and folding and irregular discontinuities in hand motion trajectories during target tracking tasks. In this regard, a new method is proposed based on compiling physiological characteristics and hand motion dynamics' geometrical traits. Thus, five tracking conditions are designed in which participants are instructed to track different target motion patterns. In these experiments, sinusoidal and trapezoidal target movements with frequencies of 0.1 and 0.3 Hz, as well as pseudo-periodic target motion created by summing two sinusoids with frequencies of 0.117 and 0.278 Hz, are used as visual targets. The results illustrate that nonuniform discontinuities are noticeable properties of the hand motion trajectory. Also, the largest Lyapunov exponent, correlation dimension, and fractal dimension corroborate that the tracking attractor is low-dimensional and chaotic. Moreover, the results are compared with the curvature-based method, and its modified version is presented by taking advantage of the proposed method. As a result, through the suggested method, stretching and folding points are well discerned regardless of discontinuities. This method can deal with the systems with intermittency in both times- and state space.

Keywords–Stretching and folding; Intermittency; Target tracking; Lyapunov Exponents; Fractal dimension; Correlation dimension.

1. INTRODUCTION

Human movement control has gained greater interest during the last decades. Craik [1] presented the hypothesis about human motor control's discrete or intermittent behavior, and Tustin [2] demonstrated early evidence of such behavior. Intermittency can also be represented during continuous tracking movements [3] and human motions [4, 5]. Such intermittency of human sensorimotor control and its discontinuities are called switching behavior and switchings [6]. Discrete and intermittent behavior of human motor control were also followed in visuo-manual tracking tasks [7, 8], and nonuniform and irregular discontinuities were reported in the hand movement trajectory during target tracking [9].

Biological systems like human movements are highly nonlinear [10]. Different studies have investigated the association between chaotic dynamics and human activities, especially in hand movements [11, 12] . Some studies have evaluated voluntary control of hand motion and its chaotic behavior during target tracking tasks [13, 14]. In contrast, others have considered the human ability to recognize chaotic target motion against randomness and predict the target's behavior over time [15, 16].

The chaotic trajectories are induced by compiling stretching and folding (SF) mechanisms [17]. Therefore, SFs, which are nonuniformly distributed in spatiotemporal space [18], can be a sign of chaotic dynamics. More precisely, stretching is a quick variation of behaviors growing in a large phase space area, whereas folding maintains the trajectory in a confined region [17] . Characterization of these two mechanisms has been considered in various fields and led to proposing multiple methods. For example, Ser-Giacomi et al. [19] investigated fluid transport within various regions of the fluid area by Lyapunov exponents (LEs). In addition, LE was used to assess the strength of stirred mixing chaoticity [20] or to evaluate the mixing quality in a planetary mixer [21]. Christov et al. [22] used SFs to evaluate the mixing deformation of fluids and showed that the first and second LE could explain the rates of SF. Souzy et al. [23] estimated the longitudinal and transverse dispersal of the porous media's velocity field by LEs. Ubeyli and Guler [24] recognized SF by positive and negative LEs, respectively. As supplementary to LEs, the asymptotic distance between nearby

trajectories was employed to quantify SF in Lorenz and Chua systems with chaotic behavior [25] or to characterize only the folding process in chaotic maps [17].

The finite-time LEs (FTLEs) algorithm has been suggested to overcome the shortcomings of the LEs algorithm. It has widely been employed to estimate the stretching mechanism in fluid mixing [26] or to specify the folding rate in the atmospheric area [27]. Also, FTLEs were adopted to determine the SF of the system's state variable [28] or fluid flow in a mixer to detect mixing quality [29]. In addition to LEs, SFs can be detected using the Poincare section and, more specifically, the return maps [30, 31], which have been broadly used to identify the chaotic dynamics of systems [32, 33]. In return maps, consecutive elongated points manifest stretching, while their convexity depicts folding. Numerous cross-sections must be considered to determine all SFs of a trajectory through the Poincare section. Due to this fact, neither FTLE-based nor Poincare section-based methods have been applied to time domain signals [27, 31]. Therefore, methods based on topological properties of the phase space trajectory have been suggested. For example, in [34, 35] SFs were characterized based on the trajectory curvature known as the curvature-based (CB) method. This method estimates an appropriate curve for a trajectory contaminated by noise using the SFs. Curves with high and low curvature were respectively regarded as folding and stretching.

This research aims to detect SFs in tracking signals obtained by performing visuo-manual tracking tasks. The task settings and descriptions, as well as the proposed method for identifying SFs, are expressed in the materials and methods section. The results section describes how the preceding procedures fail to determine SF correctly in discontinuities and also how our method overcomes the shortcomings in time and phase space. The proposed method is also compared with the CB method. The discussion section discusses the findings, and finally, the conclusion of our findings is provided in the conclusion section.

2. MATERIALS AND METHODS

2.1. Participants

Fourteen healthy subjects (14 female, right-handed, 25-32 years old) were recruited in experiments. Each participant was naive about experiments. Before beginning the experiments, informed consent, attained under the Helsinki Declaration was taken from all participants. In this consent form, some questions were asked about the participants' health condition, as well as about movement or visual deficiencies, or visuomotor pathologies. Accordingly, all participants had normal visual acuity, and none had any movement or visual deficiencies, movement disorders, remarkable neurological history, or visuomotor pathologies.

2.2. Experimental setup

Visuo-manual tracking tasks were designed and performed to evaluate the forearm's agonist and antagonist muscle activity. During target tracking tasks, participants performed wrist flexion-extension movements by propelling the joystick handle in a horizontal plane to track the visual target motions accurately. Therefore, experiments were accomplished by utilization of a computer, joystick, upper arm and forearm fixator, and a place to fix the subject's chin to avoid head movement. Eye movements should be fixed because this research concentrates on hand movement control in visuo-manual tracking tasks. To this end, the target representation window was limited on the monitor. Due to the prevention of head movements and limitations applied to the target representation window on the screen, visuomotor dynamics and eye motions could be ignored. During the experiments, participants sat on a chair 110 cm away from a monitor with their forearms fixed in two places, represented in Fig. 1 by blue stars. Also, the joystick handle was aligned with the participants' forearm, which was located on a chair handle. To evaluate forearm muscle activity, the subjects' upper limb was fixed, and shoulder and trunk movement could be disregarded accordingly. Therefore, subjects were instructed to track visual target motions utilizing a joystick handle by flexion-extension movements of their right-hand wrist in a horizontal plane. Before experiments, practice trials were performed to familiarize the participants with target tracking tasks.

2.3. Experimental procedure

The experiments were carried out in a quiet and well-lighted room. For an accurate representation of target movements, an appropriate angle of the computer screen was selected. Moreover, subjects were not fatigued before or during the experiment. Participants were instructed to carry out wrist flexion-extension movements by moving the handle in a horizontal plane to track visual target movements accurately. The target movement direction corresponds to the right and left joystick movements in a horizontal plane. Several studies have investigated the tracking procedure by demonstrating various targets, such as sinusoidal and pseudo-periodic target motions [4, 5]. In this study, sinusoidal and trapezoidal target movements with frequencies of 0.1 and 0.3 Hz, as well as pseudo-periodic target motion by summing two sinusoids with frequencies of 0.117 and 0.278 Hz, were used as visual targets in tracking tasks. According to previous studies [36, 37], participants can learn periodic/pseudo periodic target motions through visual demonstrations of targets. Learning in the context of target tracking is learning variations of target's appearance [38] or learning temporal dynamics or demonstrations of target motions [36]. Such learning is called visual learning [39] or learning target motions from visual representations [37]. To learn target's appearance by participants, the number of trials of tracking tasks and the duration of these trials should be determined so that learning periodic/pseudo-periodic target motions can be occurred [40, 41]. Consequently, each target movement, containing 18 trials with 30 seconds duration, was displayed individually. Between every two successive trials, a 30-second interval was considered a rest period. During the experiment, the position of the participant's hand motion was continuously depicted relative to the position of the target motion. This visual feedback could help subjects to compare their hand position with the target position simultaneously and lead them to track the target movements more appropriately.

2.4. Data analysis

The offline data analysis is performed using Matlab software R2018b version. It is worth noting that the determination of the occurrence of learning and analysis of tracking dynamics after transient time are of great importance. Several researchers removed tracking signals corresponding to the first 4 or 5 trials of tracking experiments to deal with transient time [42]. In contrast, other researchers considered some features to determine the occurrence of

learning and consequently tracking signals before learning was removed from investigations. For example, in [43], the reduction of tracking error was regarded as a sign of learning target motions, and tracking signals were analyzed after learning the target's appearance. Similarly, to deal with transient time in this research, a decrement in the average distance of all participants' tracking signal from the target, which leads to approaching all subjects' tracking signal to the target and reducing the tracking error, is regarded as an indicator of learning the target's appearance. In this way, transient time, that is, before the occurrence of learning, is removed from examinations.

2.5. Proposed method

SFs are striking traits of chaotic trajectories [44], such as target tracking with undetermined and nonlinear behavior [14]. Chaotic dynamics arise from the combination of SF mechanisms. During folding, the trajectory bends to hold dynamics inside a finite region of the space, while during stretching, dynamics change rapidly [17]. Also, irregular discontinuities in the time domain and phase space are observed in the hand motion trajectory. Thereby, nonuniform discontinuities and their durations are tied to tracking dynamics. Thus, a relation exists between erratic discontinuities and SF mechanisms, which has not yet been heeded in visuo-manual tracking. Here, our method is defined based on this relation, which interprets amplitude's variations to SF mechanisms according to the physiological properties of the tracking procedure. These mechanisms can be determined directly from the time domain hand motion trajectories concerning the erratic and chaotic behaviors of the target tracking.

Alternations between various mechanisms realize intermittent behavior. According to visuo-manual tracking studies, these mechanisms are the hand position specification and the target pathways' determination and prediction [45]. Therefore, tracking is initially accomplished according to the target and hand position disparity. Hence, during wrist extension, the force applied to the joystick handle was enhanced in the same direction as the target motion to track the target amplitude correctly. Afterward, to reduce the tracking error and approximate the hand movements toward the target, the applied force was increased in the opposite direction of the target motion. Therefore, tracking was performed by accelerating movements in the same and opposite direction as the target movement, respectively called positive

accelerating mechanism (PAM) and negative accelerating mechanism (NAM). As mentioned in [46], PAM and NAM can also be known as fast and slow movements.

On the other hand, SF processes are associated with the PAM and NAM in chaotic hand movement trajectories. SF's definition of chaotic orbits elucidates this relation [17]. Magnitude suddenly changes, and hand motion trajectories quickly alter during the PAM. This behavior is equivalent to the stretching trait of chaotic attractors. As a result, the points corresponding to the vertical lines of the hand motion's time series are the height of discontinuities caused by the PAM. These points are equivalent to the stretching property of the hand motion chaotic behavior [17]. In contrast, the amplitude stays unvarying during the NAM, and the trajectory locates within the finite region. This behavior is equivalent to the folding property of chaotic attractors [17]. Consequently, the points corresponding to horizontal lines of the hand motion's time series are the length of discontinuities induced by the NAM (equivalent to the folding trait). As a result, temporal discontinuities with the variable height and length in the tracking time series are caused by the alternation between the SF mechanisms. Thus, SFs can be specified based on the variation of the trajectory's amplitude over time in the hand movement time series. These discontinuities in the time series can also be observed in the phase space. According to Takens's theorem [47], the tracking attractor of each hand motion's time series is reconstructed in the phase space through computing optimum time delay and embedding dimension using the average mutual information method [48] and the false nearest neighborhood method [49], respectively. According to these methods, $P=\{x(t),x(t+\tau),x(t+2\tau),\cdots,x(t+(m-1)\tau)\}_{t=1}^{n-(m-1)\tau}$ is a reconstructed attractor in the phase space, where m and τ are the optimum embedding dimension and time delay, respectively. Each of the state vectors can be plotted against others, which results in different representations of the reconstructed attractor in phase space. Consequently, various phase space reconstructions are obtained according to the number of state vectors and the lags between these vectors, which are considered in reconstructions. Despite different reconstructions, tracking behavior and its dynamics remain unchanged in each trial of the same participants. On the other hand, as demonstrated in [50], typically, the attractor is reconstructed in 2 or 3-dimensional space, and 1τ lag between state vectors is considered. As a result, rather than considering m-dimensional space, the reconstructed phase

space of the participant's hand motion trajectory is plotted in 2D, and the 1τ lag between state vectors is regarded. For simplicity, considering

$$\begin{aligned} x &= x(t), \\ y &= x(t+\tau), \end{aligned} \tag{1}$$

the trajectory points are in the $x-y$ plane. As a result, (x, y) denotes the coordinates of each point of the phase space in the horizontal and vertical axes, respectively.

The determined SF points in the time domain are transferred to the reconstructed phase space. Consequently, the trajectory points are specified as stretching or folding according to the corresponding points in the time domain. Accordingly, points correspond to the vertical lines of the time domain tracking signals are associated with the phase space trajectory's horizontal lines. Moreover, such points correspond to where the tracking dynamics change abruptly in the phase space. Thus, they are regarded as stretching. Similarly, points corresponding to the horizontal lines of the time series belong to the points corresponding to the vertical lines in the phase space. These points are considered folding.

Discrimination of the SFs in the phase space illustrates that these properties can be specified based on geometrical features of the hand motion's chaotic behavior in the phase space. It should be noted that SFs can be determined according to the variation of the trajectory's slope. More specifically, slow-slope and high-slope points are defined as stretchings and foldings, respectively. Note that the slope of the vertical lines of the trajectory is infinite. Hence, to overcome this issue, variation of the trajectory's slope is identified through alternations of the trajectory's angle at each phase space point, determined by

$$\tan\theta = \frac{(y_2 - y_1)}{(x_2 - x_1)}, \tag{2}$$

where (x_1, y_1) and (x_2, y_2) are the coordinates of two successive points in the phase space. Equation 2 indicates that the angle at each trajectory point is calculated by the linear sum of two angles: the slope of the line connecting two consecutive points in phase space and the

angle between the horizontal line and the aforementioned connecting line. In other words, the angle at each trajectory point is derived as follows

$$\theta = \tan^{-1}\left|\frac{(y_2 - y_1)}{(x_2 - x_1)}\right| + \tan^{-1}\left|\frac{(y_3 - y_2)}{(x_3 - x_2)}\right|, \tag{3}$$

where (x_2, y_2) is the coordinates of an exemplary point with (x_1, y_1), (x_3, y_3) as the coordinates of its previous and subsequent points.

Due to the changeable and unreproducible behavior of the hand motion trajectory, the specific threshold cannot be considered to distinguish the SFs in all trials of the tracking procedure. In contrast, the angle obtained from the phase space points in each trial is regarded as a benchmark to differentiate SF for that trial. To achieve this goal, the interval between the maximum and minimum of obtained angle is divided into two parts as

$$\begin{cases} stretching & if\ \theta \le \dfrac{(\theta_{\max} + \theta_{\min})}{2} \\ folding & if\ \theta > \dfrac{(\theta_{\max} + \theta_{\min})}{2} \end{cases} \tag{4}$$

where $\theta_{\max}$ and $\theta_{\min}$ are the maximum and minimum angles in each trial. Afterward, based on the high and low angles and/or slopes, the SFs are identified. For better clarification, a flowchart of the proposed method is demonstrated in Fig. 2. As a result, the characterization of the SF by the proposed method can be plainly and easily followed.

The chaotic behavior of the hand motion trajectory has been quantified through the fractal dimension (FD). Several methods were proposed for calculating fractal dimension (FD), but some of them were employed most often, such as Higuchi's [51], Katz's [52], and Petrosian's [53] method. Among different methods of estimating the FD, Higuchi's algorithm has been extensively used during the past two decades, particularly in the analysis of biological signals [54]. This algorithm was employed in the analysis of electroencephalography (EEG) [55], electrocardiography (ECG) [56], neurons activity [57], and various neurophysiological and neuropathological studies such as detection of emotion [58], seizure onset [59], anesthesia

depth [60], anxiety [61], attention deficit hyperactivity disorder (ADHD) [62], and schizophrenia [63]. In this study, Higuchi's algorithm [51] is used to estimate the FD of the hand motion trajectories. In this method, for specific time series with successive samples $x(1), x(2), \cdots, x(N)$, where N is the total number of samples, k new time series, X_k^m is constructed from the given time series calculated as

$$X_k^m : x(m), x(m+k), x(m+2k), \cdots, x(m+\left\lfloor \frac{N-m}{k} \right\rfloor \cdot k), \tag{5}$$

for $m = 1, 2, \cdots, k$ and $k = 1, \cdots, k_{\max}$ where k is the time interval, m is the initial time, $k_{\max}$ is free adjustment parameter, and $\lfloor . \rfloor$ is the integer part of $\frac{N-m}{k}$. The length of each curve X_k^m is given by

$$L_m(k) = \frac{1}{k} \left\{ \left(\sum_{i=1}^{\left\lfloor \frac{N-m}{k} \right\rfloor} \left| x(m+ik) - x(m+(i-1)\cdot k) \right| \right) \frac{N-1}{\left\lfloor \frac{N-m}{k} \right\rfloor \cdot k} \right\}, \tag{6}$$

The term $\frac{N-1}{\left\lfloor \frac{N-m}{k} \right\rfloor \cdot k}$ is the normalization factor. The curve's length $L_m(k)$ is averaged over all m for each time interval k by the following equation

$$L(k) = \frac{1}{k} \cdot \sum_{m=1}^{k} L_m(k), \tag{7}$$

Higuchi's FD value is estimated as the slope of the straight line that fits the curve of $\ln(L(k))$ versus $\ln(1/k)$. To estimate a suitable value of the parameter $k_{\max}$, Higuchi's FD values were computed for different values of $k_{\max}$. A parameter value at which the FD approaches a

plateau is regarded as a k_{max} value [64]. In this study, Higuchi's FD is calculated with parameter $k_{max} = 300$ in all tracking conditions.

2.6. Rectification of the CB method

As previously explained, SFs are specified based on the variation of the curve orientation defined as the curvature of each trajectory point in the phase space [34, 35]. A curvature at each point is an angle between the lines connecting each point to its before and after samples. The points with low and high curvature are considered SFs. The CB method can be applied only to the phase space. It should be noted that the points corresponding to the vertical and horizontal lines of the trajectory have the same curvature. However, they arise from different mechanisms (see materials and methods section, proposed method subsection).

The CB method's deficit in the presence of discontinuities can be solved by taking advantage of the geometrical properties. These geometrical traits are used in our proposed method to discriminate between SFs. As defined in Equation 3, according to the proposed method, variations of the trajectory's angle are determined based on alternations of the trajectory's slope. Hence, the calculation of point angles should be modified in the CB method to distinguish SF points from each other in the existence of discontinuities. As a result, point angle computation is modified concerning the slope of the line connecting two successive points. Then similar to the CB method, the interval between the maximum and minimum of attained angle is divided into high and low angles regarding folding and stretching. This modified CB method can overcome the shortcomings of the original CB method facing erratic discontinuities.

3. RESULTS

3.1. Hand motion trajectories throughout target tracking tasks

Determination of the occurrence of learning and analysis of tracking dynamics after transient time are of great importance. The transient time, that is before the occurrence of learning should be removed from investigations. To deal with transient time, a decrement in the distance of the tracking signal from the target, which leads to approaching the tracking signal

to the target and reducing the tracking error, is regarded as an indicator of learning the target's appearance. The distance between these two signals is considered the Euclidean distance, which is given by [65]

$$d = \sqrt{(k_1 - x_1)^2 + (k_2 - x_2)^2 + \cdots + (k_n - x_n)^2}, \tag{8}$$

in which $(x_1, x_2, \cdots, x_n)$ and $(k_1, k_2, \cdots, k_n)$ are successive samples of the hand motion time series and target motion, respectively. Variations of the obtained distances are investigated for all participants in each trial of each tracking condition, which are demonstrated by the boxplot in Fig. 3. For better clarification, the average distances of all participants' tracking signals from the target are computed in each trial of all tracking tasks as represented by the solid red line in Fig. 3. A downtrend in the attained averages over all trials of each tracking task indicates an approximation of all participants' tracking signals to target and occurrence of learning in all subjects. In other words, a significant decrease in the average distances of all participants in one trial and, afterward, slight fluctuations of these averages in a limited range reveal that onward that trial, all participants have learned the target's appearance. This trial is represented by the green dashed line in each tracking condition in Fig. 3. As seen, learning has been occurred onward the 9th and 7th trials in all subjects during tracking periodic (part A-D in Fig. 3) and pseudo-periodic target motions (part E in Fig. 3), respectively. Also, onward the 9th and 7th trials, the average distances of all participants changed slightly in a limited range. Therefore, the 10th trial in which all participants' tracking signal passes through transient time and reaches permanent time is selected for demonstrating the results in all tracking conditions.

The hand motion trajectory is depicted in Fig. 4. During visual target tracking, the participant's hand position was continuously compared to the target. Here, PAM and NAM happen alternatively with varying durations. Alternations of duration account for error reduction at each moment and result in a declining distance between the hand movement trajectory and the target. Error decrement and variations between these two mechanisms were performed alternatively during sinusoidal target tracking compared with trapezoidal target pursuing. In contrast, error reduction occurs whenever the target's amplitude suddenly changes during tracking trapezoidal and pseudo-periodic targets compared to the sinusoidal

targets. Consequently, in this case, the PAM takes more time than the NAM. Each mechanism's duration depends on the target shape and learning its dynamics. Fig. 4 shows intermittent discontinuities that occur erratically over time in the hand motion trajectory. A phase space plot of the participant's hand motion in the 10th trial of target tracking is indicated in Fig. 5. As observed in Fig. 5, tracking patterns alter persistently over time, making the hand motion dynamic nonmonotonic, nonlinear, and unpredictable. Irregular discontinuities are also seen in the phase space trajectory.

It is worth noting that the chaotic behavior of the hand motion trajectory has also been assessed computationally by computing LEs. Chaotic behavior is quantified by this method, emphasizing the dynamical (time-dependent) aspect of the hand motion trajectories [44]. The positive value of the largest Lyapunov exponent (LLE) is typically regarded as an indicator of chaotic behavior [14]. Several methods have been employed to calculate LEs, such as [66, 67]. This study uses Kantz's algorithm [67] to compute the hand motion trajectory's LLE due to its robustness and accuracy, even for short-time trajectories. The average LLE of the hand motion trajectory (λ_{Max}) obtained over all participants is documented in Table 1 for tracking periodic and pseudo-periodic target movements. The positive values of LLE while tracking both periodic and pseudo-periodic target motions confirm the chaotic behavior of the hand motion trajectory. Also, the chaoticity of the hand motion dynamics increases as the target shape changes and the frequency rises. Compared to the periodic tracking conditions, the LLE of the tracking trajectory is more significant while tracking the pseudo-periodic target motion.

Another method for characterizing chaotic dynamics is the correlation dimension (CD). The CD is a nonlinear measure of complexity that specifies the probability that two trajectory points become close to each other within a specific distance [68]. Complexity measures can be categorized into regularity and predictability [69]. The CD is the index of predictability of a dynamical system. Different methods of quantifying predictability can be divided into two groups according to the proposed algorithm of these methods. The first group is temporal dimensionality, whereas the second one is spatial dimensionality [69]. The temporal dimensionality indices approximate the complexity of the signals directly from the time series. In contrast, the spatial dimensionality group estimate the signal's complexity through

the geometrical shape of the signals' reconstructed attractor in phase space. Consequently, the CD is the spatial dimensionality index approximating complexity in the reconstructed attractor [69, 70]. The non-integer value of the CD is a sign of chaotic behavior [71]. The average values of the CD in all tracking conditions of all participants presented in Table 1 are non-integer, indicating the chaotic behavior of the hand motion trajectories during tracking periodic and pseudo-periodic target signals. The value of the CD while tracking the sinusoidal/trapezoidal target with a frequency of 0.3 Hz is more prominent than its value for a frequency of 0.1 Hz. Also, the CD of the hand movement attractor is more significant during tracking pseudo-periodic target motion compared to tracking a sinusoidal target with a frequency of 0.1 Hz. In contrast, this value is lower than the CD of the hand motion attractor while tracking the sinusoidal target with a frequency of 0.3 Hz. As a result, as the target frequency greatens, the CD of the hand motion attractor increases according to the target shape.

The chaotic behavior of the hand motion attractor has also been quantified by the fractal dimension (FD). FD is another complexity measure, which specifies the predictability of a dynamical system. Higuchi's algorithm, which is a common method of computing FD, is a temporal dimensionality index [69] estimating the signal complexity directly in the time domain [51, 72]. In this study, the Higuchi's algorithm, which has been extensively used during the past two decades, especially in the analysis of biological signals is employed to obtain the FD values of the hand motion time series. A chaotic attractor typically holds a non-integer dimension [73]. As seen in Table 1, the average FD maintains a non-integer dimension in all tracking tasks of all participants, confirming the chaotic behavior of the hand motion trajectory. Similar to the CD, the value of the FD while tracking the sinusoidal/trapezoidal target with a frequency of 0.3 Hz is most significant than with a frequency of 0.1 Hz. Besides, this value is more prominent in pursuing pseudo-periodic target motion compared with the values of the FD while tracking any of the sinusoidal targets.

3.2. Distinction of SF by the proposed method

Target tracking is carried out by alternations between PAM and NAM with variable durations or SF mechanisms. These successive alternations result in an intermittent behavior of the tracking dynamics and nonuniform discontinuities in the hand movement behavior. The

position and duration of such discontinuities alter from one trial to another and occur irregularly that is fewer in tracking the trapezoidal target movement than the sinusoidal target motion. These discontinuities are also eliminated during tracking trapezoidal target movements with higher frequency and pseudo-periodic target motion. The PAM takes more time than the NAM by deleting sporadic discontinuities from the hand motion trajectory. The reason is that variations between these two mechanisms are accomplished according to the target shape. Consequently, as the target frequency increases, the transition between PAM and NAM becomes faster, causing the omission of discontinuities under the target configuration.

The SF points of the 10th trial of the hand motion time series and the reconstructed phase space by utilizing the proposed method are demonstrated in Figs. 6 and 7, respectively. The points corresponding to the vertical and horizontal lines of the hand motion time series are, respectively, the height (stretching) and length (folding) of discontinuities. According to the SFs definition, the phase space dynamics and the time series amplitude alter rapidly during stretching. Conversely, during folding, the phase space trajectory bends to stay inside a bounded area, and the signal's magnitude remains unvaried over time. In the time domain, the amplitude of the trajectory points corresponding to the vertical lines of the hand motion's time series changes rapidly. Thus, the points concerning the height of discontinuities in the hand movement time series are considered stretching and denoted by blue squares in Fig. 6. Moreover, the magnitude of the points associated with the horizontal line of the hand motion's time series remains unvaried over time. Hence, these points corresponding to the length of discontinuities in the hand motion time series are considered folding and denoted by green squares in Fig. 6.

The transition of the obtained SF points from the time domain trajectory to the reconstructed phase space reveals a relation between SF points in the time domain and these corresponding points in the phase space. The proposed method is wholly constructed based on the SF definition in which SF points are specified according to variations of the trajectory's angle and/or slope at phase space points. Based on the SF definition, high-slope points of the phase space trajectory wherein the trajectory bends and remains inside a finite region are considered folding and denoted by green squares in Fig. 7. Such points correspond to the vertical lines of the reconstructed attractor in the phase space. In contrast, low-slope points of the phase space

trajectory wherein the trajectory changes quickly in a broad region of the phase space are regarded as stretching and represented by blue squares in Fig. 7. Such points concern the horizontal lines of the phase space trajectory and the trajectory points wherein the dynamics vary rapidly in a large phase space area. As shown in Fig. 7, the trajectory's slope at folding points is more significant than at stretching points. Thus, the trajectory points can be specified as SF according to the variation of the point's slope. As a result of the relation between SF points in the time domain and phase space, points corresponding to the horizontal lines of the time domain signal are associated with the points of vertical lines of the phase space trajectory. In contrast, the points concerning the vertical lines of the hand movement time series correspond to the horizontal lines of the phase space trajectory and the trajectory points wherein the dynamics change quickly in the large region of the phase space.

3.3. Detection of SF by CB method and modified CB method

Here, the modified CB is examined according to the proposed method. For more clarity, in this method, the computation of the curvature, regarded as the trajectory point's angle, is modified in the CB method based on the geometrical features of the trajectory. In Figs. 8 and 9, the SF points of the 10th trial of the hand motion trajectories in phase space are depicted performing the CB method and its modified version. In these figures, the stretching and folding points are denoted by blue and green squares, respectively. For better comparison, in tracking periodic and pseudo-periodic conditions, each method's average accuracy obtained over all participants has been documented in Table 2. The accuracy is computed as

$$accuracy = \frac{(TS + TF)}{n}, \tag{9}$$

where TS and TF are the numbers of correctly characterized SF points, and n is the total points of trajectory samples.

As reported in Table 2, the variation adopted to calculate the point's angle in the modified CB method can significantly enhance the accuracy compared to the original CB method. This improvement is more significant during sinusoidal target tracking than trapezoidal and pseudo-periodic ones. In addition, the accuracy of the modified CB method is increased by

reducing the discontinuities of the hand motion. These irregular discontinuities during the sinusoidal target tracking are more than during trapezoidal and pseudo-periodic target pursuing. Therefore, the accuracy of the modified CB method is remarkably enhanced in trapezoidal and pseudo-periodic target tracking compared to the sinusoidal case. On the other hand, the CB method's accuracy is improved by reducing or omitting erratic discontinuities of the hand motion trajectory. As a result, this method has the least accuracy in the presence of discontinuities compared with other methods during the sinusoidal target tracking compared to other cases. Mathematical definitions of the proposed method match entirely the SF definition. Consequently, as represented in Table 2, the proposed method can accurately discriminate all SF points, and the accuracy is 100% in all tracking conditions. In addition, the accuracy of the proposed method is higher than the accuracy of the modified CB method during sinusoidal target tracking compared with trapezoidal and pseudo-periodic target pursuing. Overall, the identification accuracy of the proposed method is more prominent than other methods, particularly in intermittent discontinuities.

4. DISCUSSION

Target tracking was implemented by alternation between accelerating movements in the same and opposite directions as the target motion, called the PAM and NAM, respectively. The duration of each mechanism varied persistently over time and depended on the target shape and learning target dynamics. The hand motion trajectories were undetermined due to these irregular discontinuities.

In the designed experiments, learning occurred while tracking both periodic and pseudo-periodic target motions. A decrement in the distance of all participants' tracking signal from the target was regarded as a sign of learning the target's appearance. Therefore, transient time, which was before the occurrence of learning, was removed from the analysis, and tracking dynamics were analyzed after learning. On the other hand, in the hand motion trajectories, sporadic discontinuities were also observed in the presence of visual feedback from the hand motion. Miall *et al.* [74] investigated discontinuities in visual feedback from the hand motion and announced that intermittency disappeared in this situation. Huang and

Hwang [75] explained that intermittency diminished in the presence of visual feedback. These results were in contrast to our results. Indeed, the presence/absence of discontinuities in the tracking trajectory depended on the target shape and frequency. These discontinuities were fewer throughout the trapezoidal target tracking than the sinusoidal target chasing due to the similarities between the target configuration and the PAM and NAM. As the target frequency increased, these discontinuities were eliminated during trapezoidal and pseudo-periodic target tracking.

The hand motion trajectories represented nonlinear and chaotic behavior during all tracking conditions. In this research, the chaotic behavior of the hand motion trajectory has been investigated and confirmed by computing LLE throughout different tracking conditions. The average LLE of the hand motion trajectory was positive during tracking both periodic and pseudo-periodic targets, which was regarded as a sign of chaotic behavior. The predictability and chaoticity of a system were categorized by obtaining the LEs, as confirmed in [76]. In the designed experiment, the average LLE for tracking sinusoidal and trapezoidal target motions was obtained at 0.0206 ± 0.004 and 0.0296 ± 0.0014. These values were lower than the LLE during tracking pseudo-periodic target motions. Consequently, the chaoticity and unpredictability of the hand motion trajectory throughout the pseudo-periodic tracking task were more considerable than tracking either of the periodic target movements. Similar to our study, different researchers have examined the chaotic behavior of hand motion by calculating LLE during target tracking. For example, in [13], the hand motion's chaotic behavior was evaluated by calculating LLE while tracking sinusoidal and chaotic target movement in ear plethysmographs. Additionally, the values of LLE were positive in both tracking conditions, but it was more remarkable for chaotic targets than periodic signals. This result implies that the hand motion dynamics were more complicated during tracking chaotic targets. Similarly, in [14], LLE, as well as CD, was counted as a measure of chaotic behavior in the hand motion during tracking chaotic signals. The obtained values of the LLE and the CD were positive and non-integer, illustrating the hand motion's chaotic behavior. In the present study, the hand motion's chaotic behavior was also quantified by the CD and the FD. These two features are indices of predictability of a dynamical system focusing on the procedure that underlies the chaotic behavior of a system and describing the correlation that exists in the temporal evolution of that system's time series [69]. The accurate and precise

results were attained by combining Higuchi's FD and other nonlinear features [54, 58]. The combination of Higuchi's FD and CD was employed for better evaluation of muscle fatigue [77], or better differentiation of multilevel emotions [58], breathing rate [78], and disease states in multiple sclerosis, Alzheimer's and Parkinson's disease [79]. Consequently, in this study, both FD and CD were used for better investigation and comparison of tracking dynamics among different tracking tasks.

The obtained values of the CD and the FD were non-integer during all tracking tasks, indicating chaotic behavior of the hand movement trajectory. The CD explains the nonlinearity and complexity of a system, and the FD is utilized to estimate the predictability and complexity of a system, as has been discussed in [69, 76]. The lower/more significant values of these nonlinear features indicate decreased/increased complexity of dynamics of the examined signal [80]. The average CD during tracking of the sinusoidal and trapezoidal target motions was 1.1291 ± 0.0715 and 1.0644 ± 0.0138. Also, the average FD while tracking of the sinusoidal and trapezoidal target motions was 1.4646 ± 0.0403 and 1.3543 ± 0.0356. Additionally, the average CD and the FD of the hand motion attractor during tracking pseudo-periodic target motion were obtained at 1.0639 ± 0.009 and 1.7055 ± 0.0138. The average CD was the most significant value during sinusoidal target tracking. Thus, the hand motion attractor demonstrated more significant nonlinearity and complexity during tracking sinusoidal target motion. The most outstanding value of FD during chasing pseudo-periodic target motion indicated that the hand motion attractor displayed more significant unpredictability and complexity than other tracking conditions. The attained LLE, CD, and FD values suggested that the hand motion's chaotic attractor seemed low dimensional. The values of these nonlinear traits depended on the target shape and frequency. In low chaoticity of the target motion behavior, the obtained results aligned with the results expressed in [14]. This comparison between outcomes illuminated that the human hand movement represented chaotic behavior regardless of the target signal the participant tracked. Thus, the hand motion behavior can be complicated due to the target shape, but it demonstrated chaotic behavior even during tracking periodic target signals. Consequently, according to previous studies and obtained results, hand movement represented chaotic behavior while tracking any target signal, either periodic or chaotic.

On the other hand, SF features were tied to the chaotic behavior of the hand motion trajectories. SF traits were observed in tracking time series, as well as in the reconstructed attractor of the hand motion trajectories in phase space. The proposed method examined the correspondence between SF points in the time domain and phase space. This correspondence can be explained according to the definition of SF. Due to a discrepancy between the geometrical traits of the points associated with the vertical and horizontal lines of the phase space trajectory in the existence of irregular discontinuities, these points should be considered differently in systems with intermittent behavior. This fact was adopted in the proposed method by considering variations of the trajectory's angle and/or slope at phase space points, which was not included in the conventional CB method. Therefore, the accuracy obtained by the CB method was lower than the proposed method's accuracy as discontinuities in the hand motion trajectory increased. Thus, the CB method had the least accuracy when tracking sinusoidal target movements compared with pursuing trapezoidal and pseudo-periodic target motions. This method's accuracy was enhanced as the discontinuities in the hand motion were declined or omitted. Hence, the CB method was modified to address its shortcomings in erratic discontinuities. This modification was accomplished by taking advantage of the geometrical features in the phase space and could noticeably improve the method's accuracy while tracking sinusoidal targets than targeting trapezoidal and pseudo-periodic target motions. Accordingly, as discontinuities of the hand motion time series increased, the modified CB method's accuracy remarkably raised compared to the conventional CB method. Moreover, as the discontinuities of the hand motion trajectory diminished, the identification accuracy of the modified CB method approximated the proposed method's accuracy. Due to the full compliance of the proposed method with the SF definition, the accuracy of this method was noticeably more prominent than the CB method and its modified version, peculiarly in the existence of sporadic discontinuities. The proposed method can be applied to both the time domain and phase space in systems with intermittent behavior, regardless of irregular discontinuities.

5. CONCLUSION

In this research, a new method was suggested, derived from a relation between intermittent discontinuities and the stretching and folding (SF) processes in the chaotic trajectories of

target tracking. This method was proposed according to the compilation of physiological characteristics of tracking signals in the time domain and geometrical features of the hand motion trajectory in phase space. Thus, tracking dynamics have been characterized by SF features. For this concern, visuo-manual tracking experiments were designed in which participants undertook to track several periodic and pseudo-periodic target motions by moving a joystick handle. In these experiments, target tracking was carried out by wrist flexion-extension movements in a horizontal plane. Results represented that learning occurred while tracking both periodic and pseudo-periodic target motions through visual demonstrations of targets. A decrement in average distances of all participants' tracking signals from the target was regarded as an indicator of learning the target's appearance. In this way, transient time that was before the occurrence of learning was removed from examinations. In addition, nonuniform discontinuities were remarkable properties of the hand motion trajectory. These discontinuities could be manifestly observed in both time and phase domains. The number of these discontinuities and their duration constantly varied over time depending on the target shape and frequency. Also, it was found that the attractor of the hand motion trajectory was nonlinear and chaotic. Moreover, there was a relation between SF points in times- and state space. Accordingly, points corresponding to the vertical and horizontal lines of the phase space trajectory were induced by different mechanisms and should be regarded dissimilarly. This fact was considered in the proposed method by adopting variations of the hand motion trajectory's angle and/or slope at each phase space point. Conversely, it was shown that the CB method regarded the points mentioned above the same. Thus, the modification of the CB method was also presented by taking advantage of the proposed method to resolve its shortcomings in facing the nonuniform discontinuities. Overall, mathematical definitions of the proposed method match entirely the SF definition, and thereby, the proposed method could accurately distinguish all SF points in the presence and absence of discontinuities. This method can be applied to both times- and state space in systems with intermittent behavior, despite erratic discontinuities.

REFERENCES

[1] Craik, K.J. "Theory of the human operator in control systems 1: I. The operator as an engineering system", *Br. J. Psychol. Gen. Sect.,* **38**(2), pp. 56-61 (1947).

[2] Tustin, A. “The nature of the operator's response in manual control, and its implications for controller design”, *J. Inst. Elec. Eng., Part IIA,* **94**(2), pp. 190-206 (1947).

[3] Susilaradeya, D., Xu, W., Hall, T.M., et al. “Extrinsic and intrinsic dynamics in movement intermittency”, *Elife,* **8**, p. e40145 (2019).

[4] Stark, L. “Neurological control systems: Studies in bioengineering”: Springer Science & Business Media (2012).

[5] Sakaguchi, Y., Tanaka, M., and Inoue, Y. “Adaptive intermittent control: a computational model explaining motor intermittency observed in human behavior”, *Neural Netw.,* **67**, pp. 92-109 (2015).

[6] Nema, S., Kowalczyk, P., and Loram, I. “Wavelet-frequency analysis for the detection of discontinuities in switched system models of human balance”, *Hum. Mov. Sci.,* **51**, pp. 27-40 (2017).

[7] Gollee, H., Gawthrop, P.J., Lakie, M., et al. “Visuo- manual tracking: does intermittent control with aperiodic sampling explain linear power and non- linear remnant without sensorimotor noise?”, *J. Physiol.,* **595**(21), pp. 6751-6770 (2017).

[8] Choi, W., Lee, J., Yanagihara, N., et al. “Development of a quantitative evaluation system for visuo-motor control in three-dimensional virtual reality space”, *Sci. Rep.,* **8**(1), pp. 1-9 (2018).

[9] Sakaguchi, Y. “Intermittent brain motor control observed in continuous tracking task”, In *Advances in cognitive neurodynamics (III)*, Edn., pp. 461-468, Springer (2013).

[10] Rahatabad, F.N., Fallah, A., and Jafari, A.H. “A study of chaotic phenomena in human-like reaching movements”, *Int. J. Bifurcat. Chaos,* **21**(11), pp. 3293-3303 (2011).

[11] Josiński, H., Grabiec, P., Pawlyta, M., et al. “Analysis of chaotic behaviors in gait of the elderly using the CAREN extended system”, *IEEE 20th Healthcom*, pp. 1-6 (2018).

[12] Lee, J., Guo, Y., Ravikumar, V., et al. “Towards the Development of Nonlinear Approaches to Discriminate AF from NSR Using a Single-Lead ECG”, *Entropy,* **22**(5), p. 531 (2020).

[13] Miao, T., Shimizu, T., Makabe, H., et al. “Chaos in ear plethysmograms: Tracking experiment and a model”, *Conf. Proc. IEEE Int. Conf. Syst. Man Cybern.*, pp. 2982-2987 (2008).

[14] Takagi, A., Furuta, R., Saetia, S., et al. “Behavioral and physiological correlates of kinetically tracking a chaotic target”, *PLoS One,* **15**(9), p. e0239471 (2020).

[15] Dotov, D. and Froese, T. “Entraining chaotic dynamics: a novel movement sonification paradigm could promote generalization”, *Hum. Mov. Sci.,* **61**, pp. 27-41 (2018).

[16] Stepp, N. “Anticipation in feedback-delayed manual tracking of a chaotic oscillator”, *Exp. Brain Res.,* **198**(4), pp. 521-525 (2009).

[17] Baran, V., Zus, M., Bonasera, A., et al. “Quantifying the folding mechanism in chaotic dynamics”, *Rom. J. Phys.,* **60**, pp. 1263-77 (2015).

[18] Ma, T., Ouellette, N.T., and Bollt, E.M. “Stretching and folding in finite time”, *Chaos: Interdiscipl. J. Nonlinear Sci.,* **26**(2), p. 023112 (2016).

[19] Ser-Giacomi, E., Rossi, V., López, C., et al. “Flow networks: A characterization of geophysical fluid transport”, *Chaos: Interdiscipl. J. Nonlinear Sci.,* **25**(3), p. 036404 (2015).

[20] Huang, Y., Dehkordy, F.M., Li, Y., et al. “Enhancing anaerobic fermentation performance through eccentrically stirred mixing: Experimental and modeling methodology”, *Chem. Eng. J.*, **334**, pp. 1383-1391 (2018).

[21] Mostefa, T., Eddine, A.D., Tayeb, N.T., et al. “Kinematic Properties of a Twisted Double Planetary Chaotic Mixer: A Three-Dimensional Numerical Investigation”, *Micromachines*, **13**(9), p. 1545 (2022).

[22] Christov, I.C., Lueptow, R.M., and Ottino, J.M. “Stretching and folding versus cutting and shuffling: An illustrated perspective on mixing and deformations of continua”, *Am. J. Phys.*, **79**(4), pp. 359-367 (2011).

[23] Souzy, M., Lhuissier, H., Méheust, Y., et al. “Velocity distributions, dispersion and stretching in three-dimensional porous media”, *J. Fluid Mech.*, **891**, p. A16 (2020).

[24] Ubeyli, E.D. and Guler, İ. “Statistics over Lyapunov exponents for feature extraction: electroencephalographic changes detection case”, *World Enform. Soc.*, **2**, pp. 169-172 (2004).

[25] Bonasera, A., Bucolo, M., Fortuna, L., et al. “Experimental Evaluation Of The d∞ Parameter to Characterize Chaotic Dynamics”, *AIP Conf. Proc.*, pp. 355-362 (2003).

[26] Ahmad, R., Farooqi, A., Zhang, J., et al. “Analysis of Transport and Mixing Phenomenon to Invariant Manifolds Using LCS and KAM Theory Approach in Unsteady Dynamical Systems”, *IEEE Access*, **8**, pp. 141057-141065 (2020).

[27] MP Perez, G., Vidale, P.L., Klingaman, N.P., et al. “Atmospheric convergence zones stemming from large-scale mixing”, *Weather Clim. Dynam. Discuss*, pp. 1-22 (2020).

[28] Suresh, K., Prasad, A., and Thamilmaran, K. “Birth of strange nonchaotic attractors through formation and merging of bubbles in a quasiperiodically forced Chua’ s oscillator”, *Phys. Lett. A*, **377**(8), pp. 612-621 (2013).

[29] Younes, E., Moguen, Y., El Omari, K., et al. “Experimental study of chaotic flow and mixing of Newtonian fluid in a rotating arc-wall mixer”, *Int. J. Heat Mass Transf.*, **187**, p. 122459 (2022).

[30] Rössler, O.E. and Letellier, C. “Chaos: The World of Nonperiodic Oscillations”: Springer Nature (2020).

[31] Chen, S., Hao, M., Shang, J., et al. “Numerical analysis of modified micromixers with staggered E-shape mixing units”, *Chem. Eng. Process*, **179**, p. 109087 (2022).

[32] Clemente-López, D., Tlelo-Cuautle, E., de la Fraga, L.-G., et al. “Poincaré maps for detecting chaos in fractional-order systems with hidden attractors for its Kaplan-Yorke dimension optimization”, *AIMS Math.*, **7**(4), pp. 5871-5894 (2022).

[33] Xie, J., Wang, Y., and Tang, B. “Chaotic dynamics of string around the Bardeen-AdS black holes surrounded by quintessence dark energy”, *arXiv:2210.08641*, (2022).

[34] Jafari, S., Golpayegani, S.H., and Jafari, A. “A novel noise reduction method based on geometrical properties of continuous chaotic signals”, *Sci. Iran.*, **19**(6), pp. 1837-1842 (2012).

[35] Molaie, M., Jafari, S., Moradi, M.H., et al. “A chaotic viewpoint on noise reduction from respiratory sounds”, *Biomed. Signal Process. Control*, **10**, pp. 245-249 (2014).

[36] Yang, Y., Liu, X., Wu, J., et al. “SimPer: Simple Self-Supervised Learning of Periodic Targets”, *arXiv:2210.03115*, (2022).

[37] Yang, J., Zhang, J., Settle, C., et al. “Learning periodic tasks from human demonstrations”, *IEEE Int. Conf. Robot. Autom. (ICRA)*, pp. 8658-8665 (2022).

[38] Guo, Q., Feng, W., Zhou, C., et al. “Learning dynamic siamese network for visual object tracking”, *Proc. IEEE Int. Conf. Comput. Vis.*, pp. 1763-1771 (2017).

[39] Makovski, T., Vazquez, G.A., and Jiang, Y.V. “Visual learning in multiple-object tracking”, *PLoS One*, **3**(5), p. e2228 (2008).

[40] Mathew, J., Eusebio, A., and Danion, F. “Limited contribution of primary motor cortex in eye-hand coordination: a TMS study”, *J. Neurosci.*, **37**(40), pp. 9730-9740 (2017).

[41] Bank, P.J., Dobbe, L.R., Meskers, C.G., et al. “Manipulation of visual information affects control strategy during a visuomotor tracking task”, *Behav. Brain Res.*, **329**, pp. 205-214 (2017).

[42] Maiello, G., Kwon, M., and Bex, P.J. “Three-dimensional binocular eye–hand coordination in normal vision and with simulated visual impairment”, *Exp. Brain Res.*, **236**, pp. 691-709 (2018).

[43] Parker, M.G., Willett, A.B., Tyson, S.F., et al. “A systematic evaluation of the evidence for Perceptual Control Theory in tracking studies”, *Neurosci. Biobehav. Rev.*, **112**, pp. 616-633 (2020).

[44] Hilborn, R.C. “Chaos and nonlinear dynamics: an introduction for scientists and engineers”: Oxford University Press on Demand (2000).

[45] Patterson, J.R., Brown, L.E., Wagstaff, D.A., et al. “Limb position drift results from misalignment of proprioceptive and visual maps”, *J. Neurosci.*, **346**, pp. 382-394 (2017).

[46] Guigon, E., Chafik, O., Jarrasse, N., et al. “Experimental and theoretical study of velocity fluctuations during slow movements in humans”, *J. Neurophysiol.*, **121**(2), pp. 715-727 (2019).

[47] Takens, F. “Detecting strange attractors in turbulence”, In *Dynamical systems and turbulence, Warwick 1980*, Edn., pp. 366-381, Springer (1981).

[48] Liebert, W. and Schuster, H. “Proper choice of the time delay for the analysis of chaotic time series”, *Phys. Lett. A*, **142**(2-3), pp. 107-111 (1989).

[49] Kennel, M.B., Brown, R., and Abarbanel, H.D. “Determining embedding dimension for phase-space reconstruction using a geometrical construction”, *Phys. Rev. A*, **45**(6), p. 3403 (1992).

[50] de Pedro-Carracedo, J., Fuentes-Jimenez, D., Ugena, A.M., et al. “Phase space reconstruction from a biological time series: A photoplethysmographic signal case study”, *Appl. Sci.*, **10**(4), p. 1430 (2020).

[51] Higuchi, T. “Approach to an irregular time series on the basis of the fractal theory”, *Physica D*, **31**(2), pp. 277-283 (1988).

[52] Katz, M.J. “Fractals and the analysis of waveforms”, *Comput. Biol. Med.*, **18**(3), pp. 145-156 (1988).

[53] Petrosian, A. “Kolmogorov complexity of finite sequences and recognition of different preictal EEG patterns”, *Proc. eighth IEEE Symp. Comput.-Based Med. Syst.*, pp. 212-217 (1995).

[54] Kesić, S. and Spasić, S.Z. “Application of Higuchi's fractal dimension from basic to clinical neurophysiology: A review”, *Comput. Methods Programs Biomed.*, **133**, pp. 55-70 (2016).

[55] Yazdi-Ravandi, S., Arezooji, D.M., Matinnia, N., et al. “Complexity of information processing in obsessive-compulsive disorder based on fractal analysis of EEG signal”, *EXCLI J.*, **20**, p. 642 (2021).

[56] Sharanya, S. and Arjunan, S.P. “FRACTAL DIMENSION TECHNIQUES FOR ANALYSIS OF CARDIAC AUTONOMIC NEUROPATHY (CAN)”, *Biomed. Eng. (Singapore),* p. 2350003 (2023).

[57] Vivekanandhan, G., Mehrabbeik, M., Rajagopal, K., et al. “Higuchi fractal dimension is a unique indicator of working memory content represented in spiking activity of visual neurons in extrastriate cortex”, *Math. Biosci. Eng.,* **20**(2), pp. 3749-3767 (2022).

[58] Sharma, K., Dash, A., and Kumar, D. “Investigating the Effect of EEG Channel Selection on Inter-subject Emotion Classification”, *13th Int. Conf. Cloud Comput. Data Sci. Eng.*, pp. 312-316 (2023).

[59] Amiri, M., Aghaeinia, H., and Amindavar, H.R. “Automatic epileptic seizure detection in EEG signals using sparse common spatial pattern and adaptive short-time Fourier transform-based synchrosqueezing transform”, *Biomed. Signal Process. Control,* **79**, p. 104022 (2023).

[60] Negahbani, E., Amirfattahi, R., Ahmadi, B., et al. “Electroencephalogram Fractral Dimension as a Measure of Depth of Anesthesia”, *3rd Int. Conf. Inf. Commun. Technol. : Theory Appl.*, pp. 1-5 (2008).

[61] Minkowski, L., Mai, K.V., and Gurve, D. “Feature Extraction to Identify Depression and Anxiety Based on EEG”, *43rd Annu. Int. Conf. IEEE Eng. Med. Biol. Soc . (EMBC),* pp. 6322-6325 (2021).

[62] Alim, A. and Imtiaz, M.H. “Automatic Identification of Children with ADHD from EEG Brain Waves”, *Signals,* **4**(1), pp. 193-205 (2023).

[63] de Miras, J.R., Ibáñez-Molina, A., Soriano, M., et al. “Schizophrenia classification using machine learning on resting state EEG signal”, *Biomed. Signal Process. Control,* **79**, p. 104233 (2023).

[64] Wanliss, J. and Wanliss, G.E. “Efficient calculation of fractal properties via the Higuchi method”, *Nonlinear Dyn.,* **109**(4), pp. 2893-2904 (2022).

[65] Wang, B., Liu, X., Yu, B., et al. “An improved WiFi positioning method based on fingerprint clustering and signal weighted Euclidean distance”, *Sensors,* **19**(10), p. 2300 (2019).

[66] Kuznetsov, N., Alexeeva, T., and Leonov, G. “Invariance of Lyapunov exponents and Lyapunov dimension for regular and irregular linearizations”, *Nonlinear Dyn.,* **85**(1), pp. 195-201 (2016).

[67] Kantz, H. “A robust method to estimate the maximal Lyapunov exponent of a time series”, *Phys. Lett. A,* **185**(1), pp. 77-87 (1994).

[68] Rampichini, S., Vieira, T.M., Castiglioni, P., et al. “Complexity analysis of surface electromyography for assessing the myoelectric manifestation of muscle fatigue: A review”, *Entropy,* **22**(5), p. 529 (2020).

[69] Lau, Z.J., Pham, T., Chen, S.A., et al. “Brain entropy, fractal dimensions and predictability: A review of complexity measures for EEG in healthy and neuropsychiatric populations”, *Eur. J. Neurosci.,* **56**(7), pp. 5047-5069 (2022).

[70] Grebogi, C., Ott, E., and Yorke, J.A. “Critical exponent of chaotic transients in nonlinear dynamical systems”, *Phys. Rev. Lett.,* **57**(11), p. 1284 (1986).

[71] Hirata, Y., Oda, A.H., Motono, C., et al. “Imputation-free reconstructions of three-dimensional chromosome architectures in human diploid single-cells using allele-specified contacts”, *Sci. Rep.,* **12**(1), pp. 1-10 (2022).

[72] Spasić, S. “Surrogate data test for nonlinearity of the rat cerebellar electrocorticogram in the model of brain injury”, *Signal Process.,* **90**(12), pp. 3015-3025 (2010).

[73] Ahmad, S., Ullah, A., and Akgül, A. “Investigating the complex behaviour of multi-scroll chaotic system with Caputo fractal-fractional operator”, *Chaos Solitons Fractals*, **146**, p. 110900 (2021).

[74] Miall, R.C., Weir, D., and Stein, J. “Intermittency in human manual tracking tasks”, *J. Mot. Behav.*, **25**(1), pp. 53-63 (1993).

[75] Huang, C.-T. and Hwang, S. “Eye-hand synergy and intermittent behaviors during target-directed tracking with visual and non-visual information”, *PLoS One*, **7**(12), p. e51417 (2012).

[76] Rashidi, S., Fallah, A., and Towhidkhah, F. “Nonlinear analysis of dynamic signature”, *Indian J. Phys.*, **87**(12), pp. 1251-1261 (2013).

[77] Fegni Ndam, E.O., Goubault, E., Moyen-Sylvestre, B., et al. “What are the best indicators of myoelectric manifestation of fatigue?”, *medRxiv*, p. 2023.03. 02.23286583 (2023).

[78] Mayor, D., Steffert, T., Datseris, G., et al. “Complexity and Entropy in Physiological Signals (CEPS): Resonance Breathing Rate Assessed Using Measures of Fractal Dimension, Heart Rate Asymmetry and Permutation Entropy”, *Entropy*, **25**(2), p. 301 (2023).

[79] Garehdaghi, F. and Sarbaz, Y. “Analyzing global features of magnetic resonance images in widespread neurodegenerative diseases: new hope to understand brain mechanism and robust neurodegenerative disease diagnosis”, *Med. Biol. Eng. Comput.*, pp. 1-12 (2023).

[80] Chandrasekharan, S., Jacob, J.E., Cherian, A., et al. “Exploring recurrence quantification analysis and fractal dimension algorithms for diagnosis of encephalopathy”, *Cogn. Neurodyn.*, pp. 1-14 (2023).

Fig. 1. Forearm fixing places in tracking experiments. As depicted by the blue stars, the participant's forearm is fixed in two areas to prevent its movements and provide only wrist flexion-extension motions in the horizontal plane.

Fig. 2. Flowchart of the proposed method. The proposed method is constructed based on the stretching and folding (SF) definition in which SF points are specified according to variations of the trajectory's angle and/or slope at each phase space point. High-slope points wherein the trajectory bends and remains inside a finite region are considered folding. In contrast, low-slope points wherein the trajectory changes quickly in a large phase space area are regarded as stretching.

Fig. 3. Box plot of Euclidean distances of all participants' tracking signal from target in each trial while tracking three types of target motion: A, B) sinusoidal with a frequency of 0.1 Hz and 0.3 Hz, C, D) trapezoidal with a frequency of 0.1 Hz and 0.3 Hz, and E) pseudo-periodic target motion created by summing two sinusoids with frequencies of 0.117 Hz and 0.278 Hz. The average distances of all participants' signals from the target are represented by the solid red line and a decrement in these distances is regarded as an indicator of learning the target's appearance. A trial in which a significant decrease is observed in the average distances is demonstrated by green dashed lines. After this trial, the average distances changed slightly in a limited range.

Fig. 4. Participants' hand motion time series in the 10th trial of tracking three types of target motion: A, B) sinusoidal with a frequency of 0.1 Hz and 0.3 Hz, C, D) trapezoidal with a frequency of 0.1 Hz and 0.3 Hz, and E) pseudo-periodic target motion created by summing two sinusoids with frequencies of 0.117 Hz and 0.278 Hz. Hand and target movements are shown with solid and dashed lines, respectively. Nonuniform discontinuities that alternate between positive accelerating mechanism (PAM) and negative accelerating mechanism (NAM) are observed in tracking signals. As the target frequency increases, the transition between PAM and NAM becomes faster, causing the decrement or omission of discontinuities under the target configuration.

Fig. 5. Reconstructed phase space of the participants' hand motion trajectory for the 10th trial of target tracking experiments with three types of target motion: A, B) sinusoidal with a frequency of 0.1 Hz ($\tau = 17$) and 0.3 Hz ($\tau = 11$), C, D) trapezoidal with a frequency of 0.1 Hz ($\tau = 6$) and 0.3 Hz ($\tau = 3$), and E) pseudo-periodic target motion created by summing two sinusoids with frequencies of 0.117 Hz and 0.278 Hz ($\tau = 4$). Nonuniform discontinuities are observed in the phase space. These discontinuities decrease as the target frequency increases. The target tracking dynamic is nonlinear, non-repetitive, and unpredictable.

Fig. 6. Stretching and folding (SF) points of the participant's hand motion time series in the 10th trial of tracking experiments detected by the proposed method with three types of target motion: A, B) sinusoidal with a frequency of 0.1 Hz and 0.3 Hz, C, D) trapezoidal with a frequency of 0.1 Hz and 0.3 Hz, and E) pseudo-periodic target motion created by summing two sinusoids with frequencies of 0.117 Hz and 0.278 Hz. Trajectory's amplitude at points corresponding to the vertical lines of the time domain signal varies rapidly. These points are considered stretching and represented by blue squares. Conversely, the amplitude remains

unchanged at points corresponding to the horizontal lines. These points are regarded as folding and depicted by green squares.

Fig. 7. Stretching and folding (SF) points of the reconstructed hand motion trajectory in the 10th trial of tracking experiments detected by the proposed method with three types of target motion: A, B) sinusoidal with a frequency of 0.1 Hz ($\tau = 17$) and 0.3 Hz ($\tau = 11$), C, D) trapezoidal with a frequency of 0.1 Hz ($\tau = 6$) and 0.3 Hz ($\tau = 3$), and E) pseudo-periodic target motion created by summing two sinusoids with frequencies of 0.117 Hz and 0.278 Hz ($\tau = 4$). High-slope points are considered folding and represented by green squares, whereas low-slope points are regarded as stretching and demonstrated by blue squares. The points corresponding to the vertical and horizontal lines of the trajectory differ.

Fig. 8. Stretching and folding (SF) points of the reconstructed hand motion trajectory in the 10th trial of tracking experiments detected by the curvature-based (CB) method with three types of target motion: A, B) sinusoidal with a frequency of 0.1 Hz ($\tau = 17$) and 0.3 Hz ($\tau = 11$), C, D) trapezoidal with a frequency of 0.1 Hz ($\tau = 6$) and 0.3 Hz ($\tau = 3$), and E) pseudo-periodic target motion created by summing two sinusoids with frequencies of 0.117 Hz and 0.278 Hz ($\tau = 4$). High-curvature points are considered folding and represented by green squares, whereas low-curvature ones are regarded as stretching and represented by blue squares. The points of horizontal and vertical lines of the trajectory have the same angle and are considered quite similar, although they arise from different mechanisms.

Fig. 9. Stretching and folding (SF) points of the reconstructed hand motion trajectory in the 10th trial of tracking experiments detected by the modified curvature-based (CB) method with three types of target motion: A, B) sinusoidal with a frequency of 0.1 Hz ($\tau = 17$) and 0.3 Hz ($\tau = 11$), C, D) trapezoidal with a frequency of 0.1 Hz ($\tau = 6$) and 0.3 Hz ($\tau = 3$), and E) pseudo-periodic target motion created by summing two sinusoids with frequencies of 0.117 Hz and 0.278 Hz ($\tau = 4$). The computation of the angle at each point is modified by taking advantage of the proposed method. This modified CB method can overcome the shortcomings of the original CB method facing erratic discontinuities. Blue and green squares represent the SF points.

Table 1. The average correlation dimension (CD), fractal dimension (FD), and largest Lyapunov exponent (LLE) of hand motion trajectories using different targets were obtained over all participants after the occurrence of learning ($\text{mean} \pm \text{sd}$). These features are calculated for all participants' trajectories from the 10th trial onward in all tracking conditions. The positive values of LLE and non-integer values of CD and FD in both periodic and pseudo-periodic target motions indicate the chaotic behavior of tracking trajectories. The LLE increases as the target shape changes and the frequency rises. CD and FD are greater during tracking sinusoidal/trapezoidal targets with a frequency of 0.3 Hz than with a frequency of 0.1 Hz.

Table 2. Accuracy of the proposed method, curvature-based (CB), and modified CB methods using different targets obtained over all participants after the occurrence of learning ($\text{mean}\% \pm \text{sd}\%$). The accuracy is

calculated from the 10th trial onward through all methods. The CB method has the least accuracy compared to other methods, especially in the presence of discontinuities during tracking sinusoidal targets compared to other cases. Modification of the CB method can significantly increase the accuracy, particularly during tracking sinusoidal target motions. Despite this improvement in the modified CB method's accuracy, the proposed method’s accuracy is more prominent than other methods, particularly in facing intermittent discontinuities.

Fig. 1.

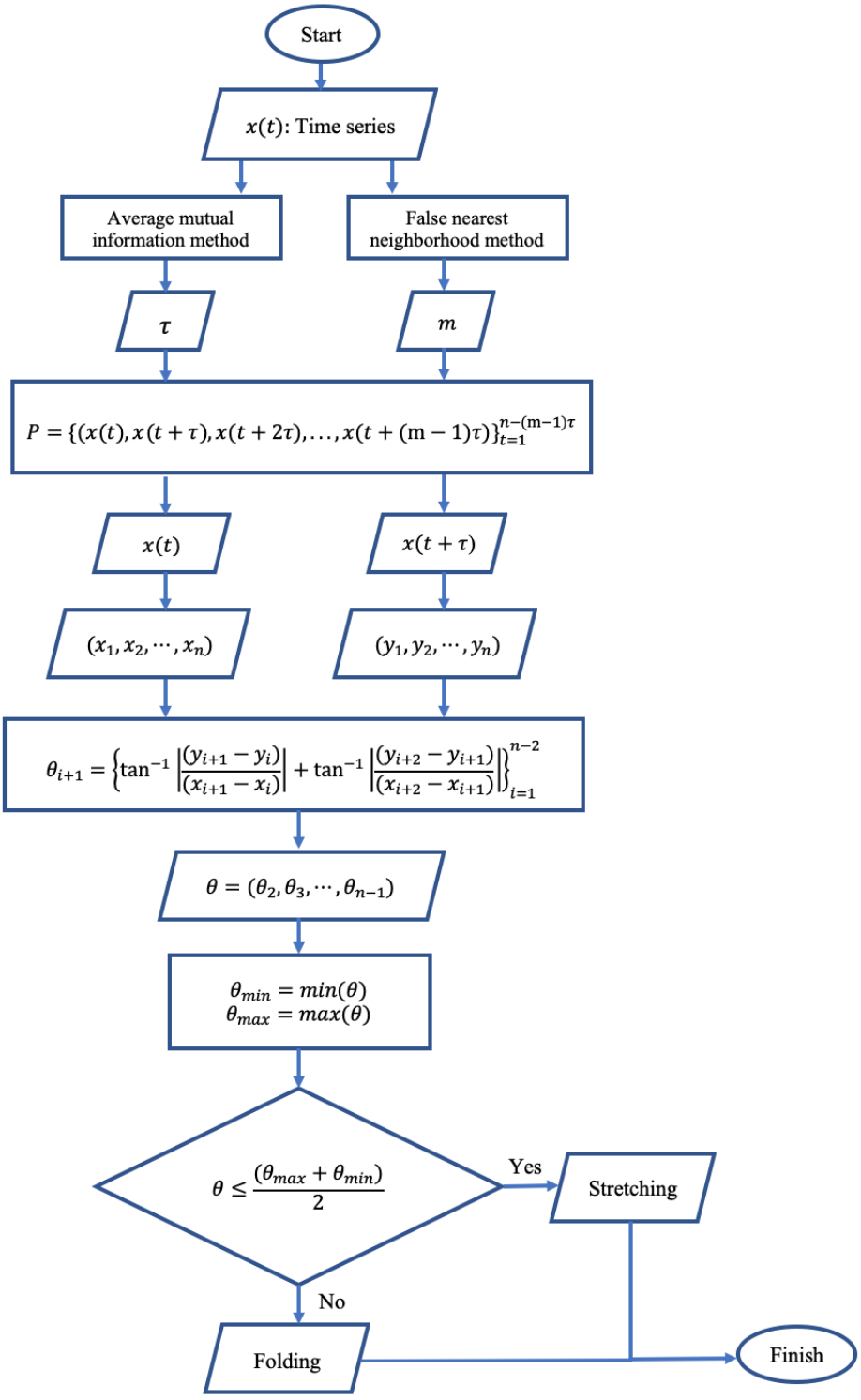
Start
$x(t)$: Time series
Average mutual information method
False nearest neighborhood method
τ
m
$P = \{(x(t), x(t+\tau), x(t+2\tau), \ldots, x(t+(\mathrm{m}-1)\tau)\}_{t=1}^{n-(\mathrm{m}-1)\tau}$
$x(t)$
$x(t+\tau)$
$(x_1, x_2, \cdots, x_n)$
$(y_1, y_2, \cdots, y_n)$
$\theta_{i+1} = \left\{\tan^{-1}\left|\frac{(y_{i+1}-y_i)}{(x_{i+1}-x_i)}\right| + \tan^{-1}\left|\frac{(y_{i+2}-y_{i+1})}{(x_{i+2}-x_{i+1})}\right|\right\}_{i=1}^{n-2}$
$\theta = (\theta_2, \theta_3, \cdots, \theta_{n-1})$
$\theta_{min} = min(\theta)$
$\theta_{max} = max(\theta)$
$\theta \leq \frac{(\theta_{max}+\theta_{min})}{2}$
Yes
Stretching
No
Folding
Finish

Fig. 2.

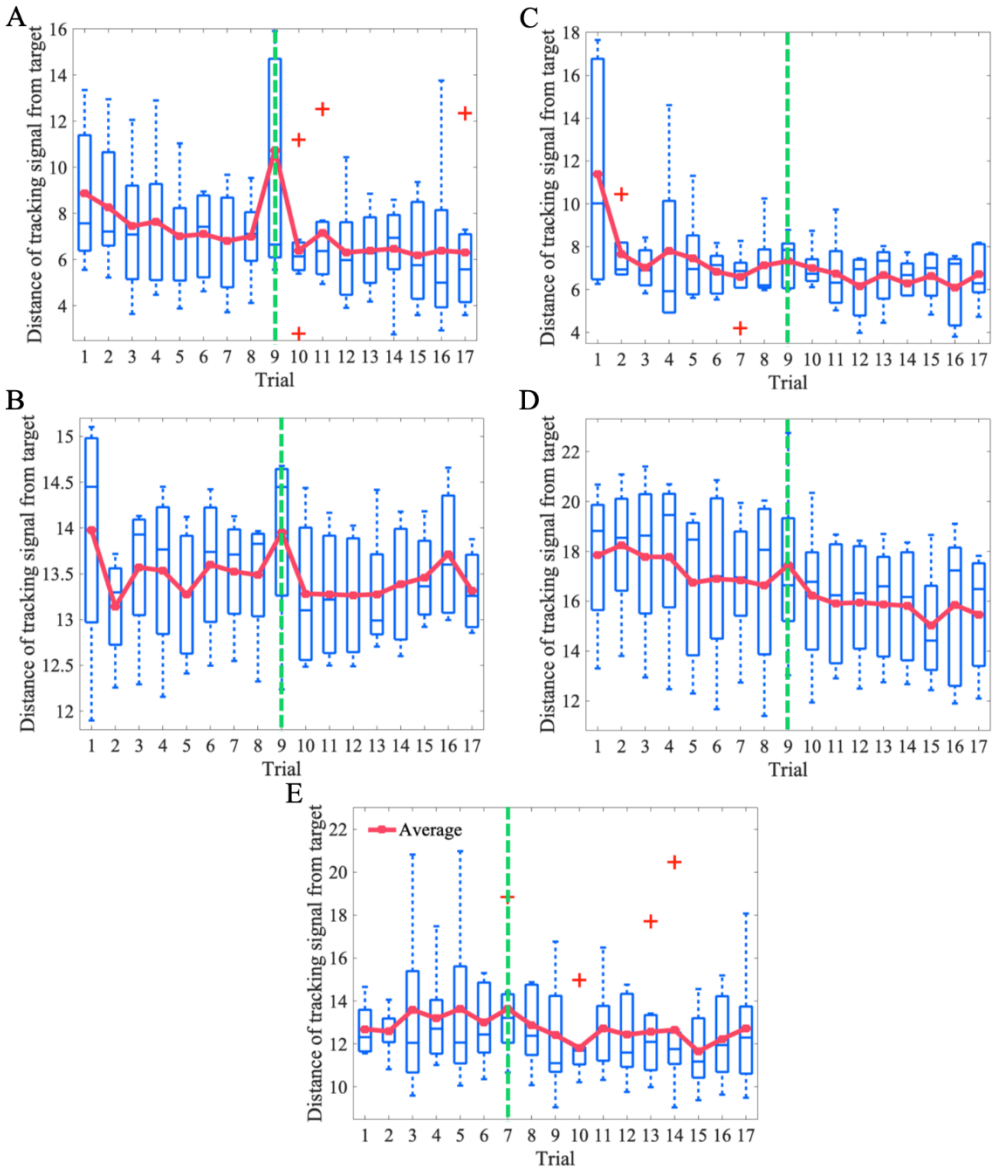
A
Distance of tracking signal from target
Trial
C
Distance of tracking signal from target
Trial
B
Distance of tracking signal from target
Trial
D
Distance of tracking signal from target
Trial
E
Average
Distance of tracking signal from target
Trial

Fig. 3.

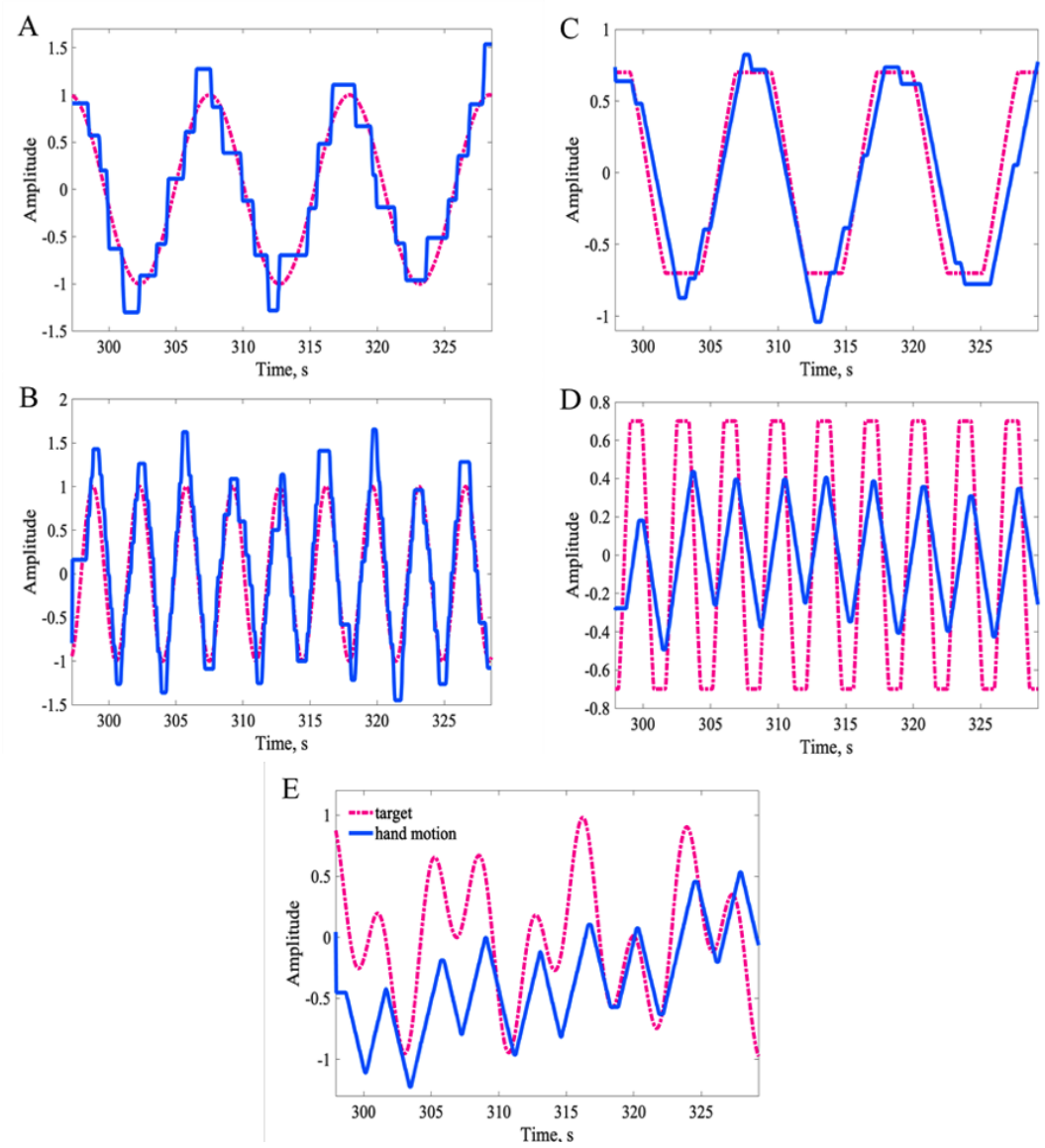

Fig. 4.

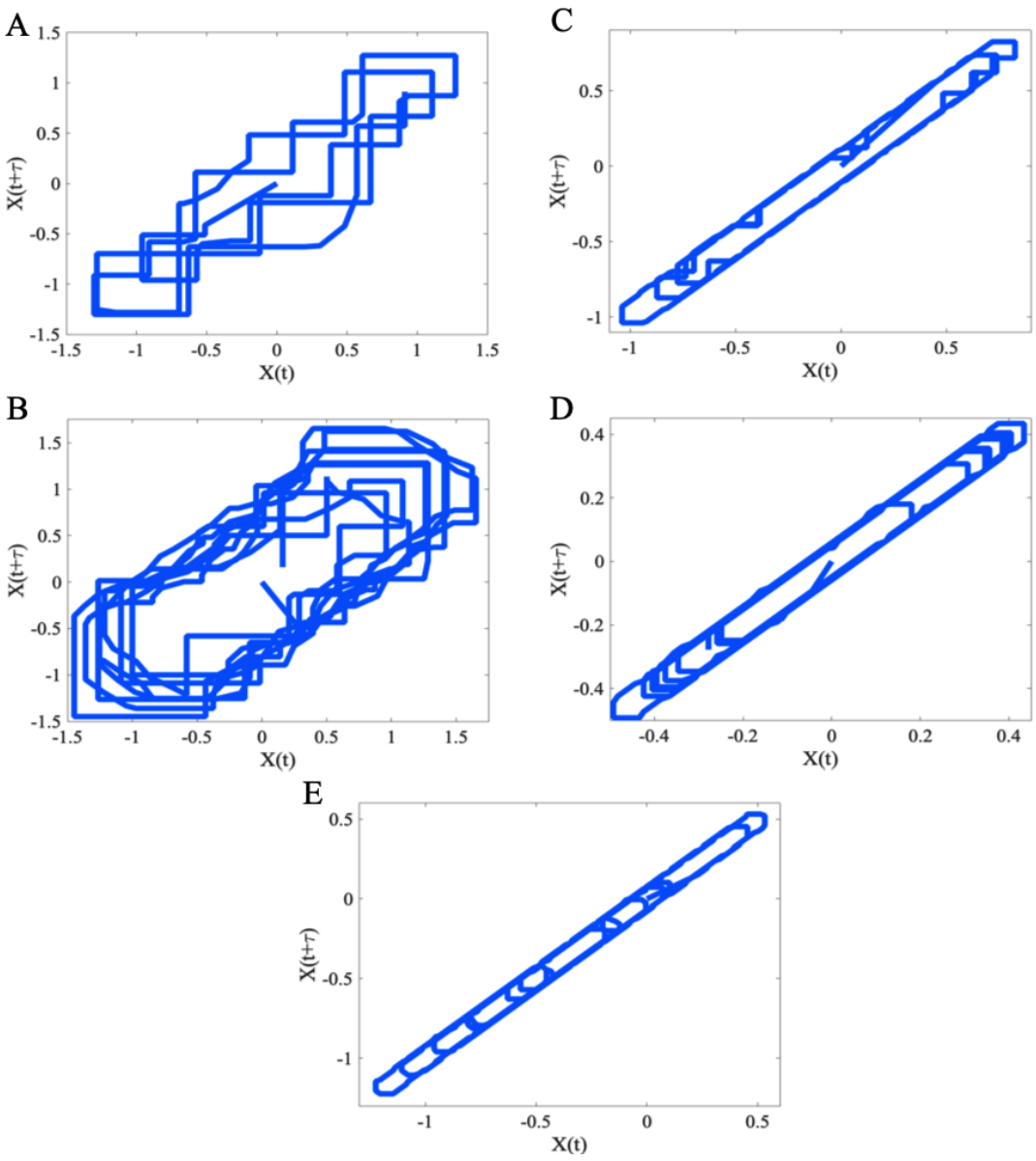

Fig. 5.

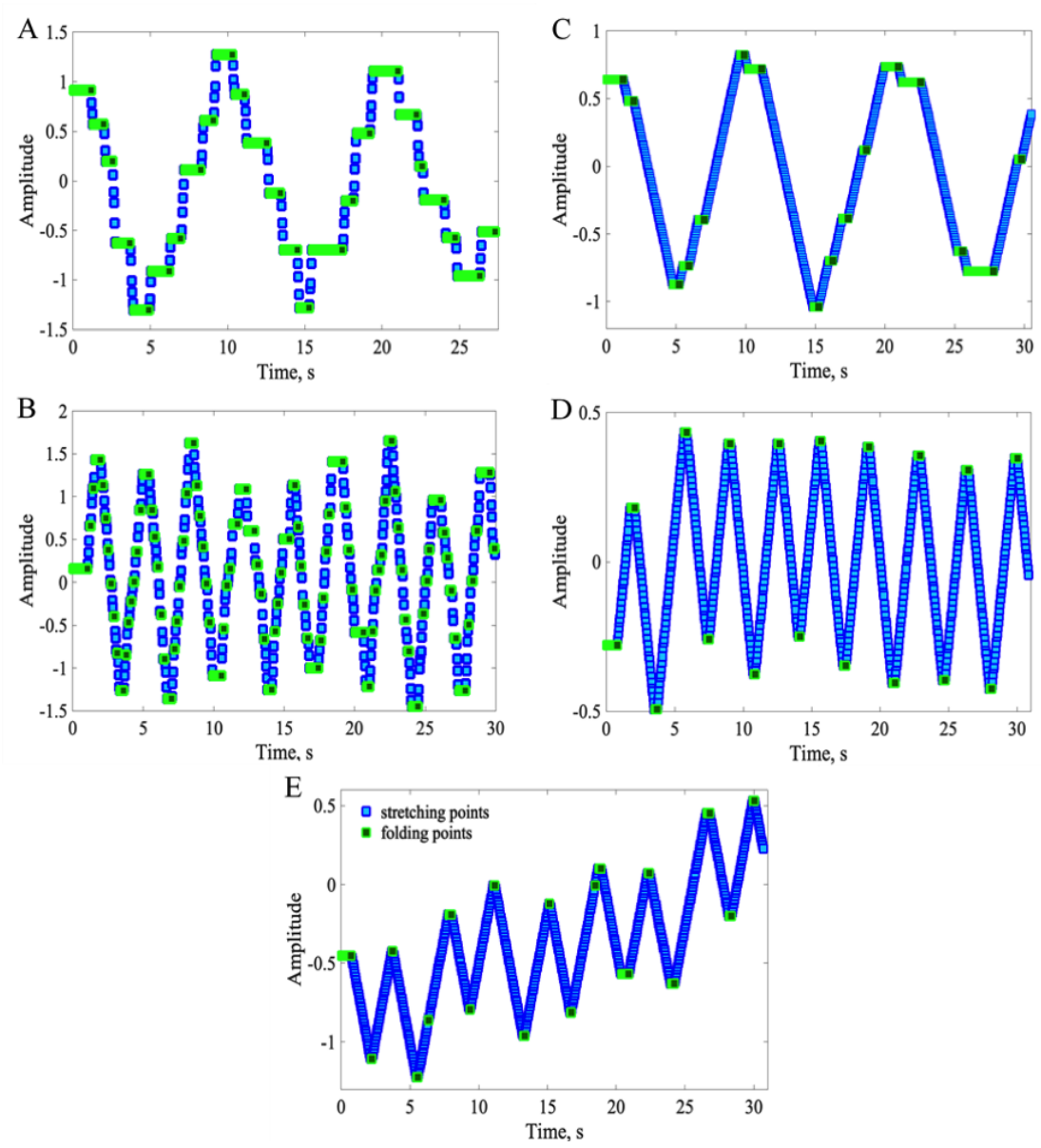

Fig. 6.

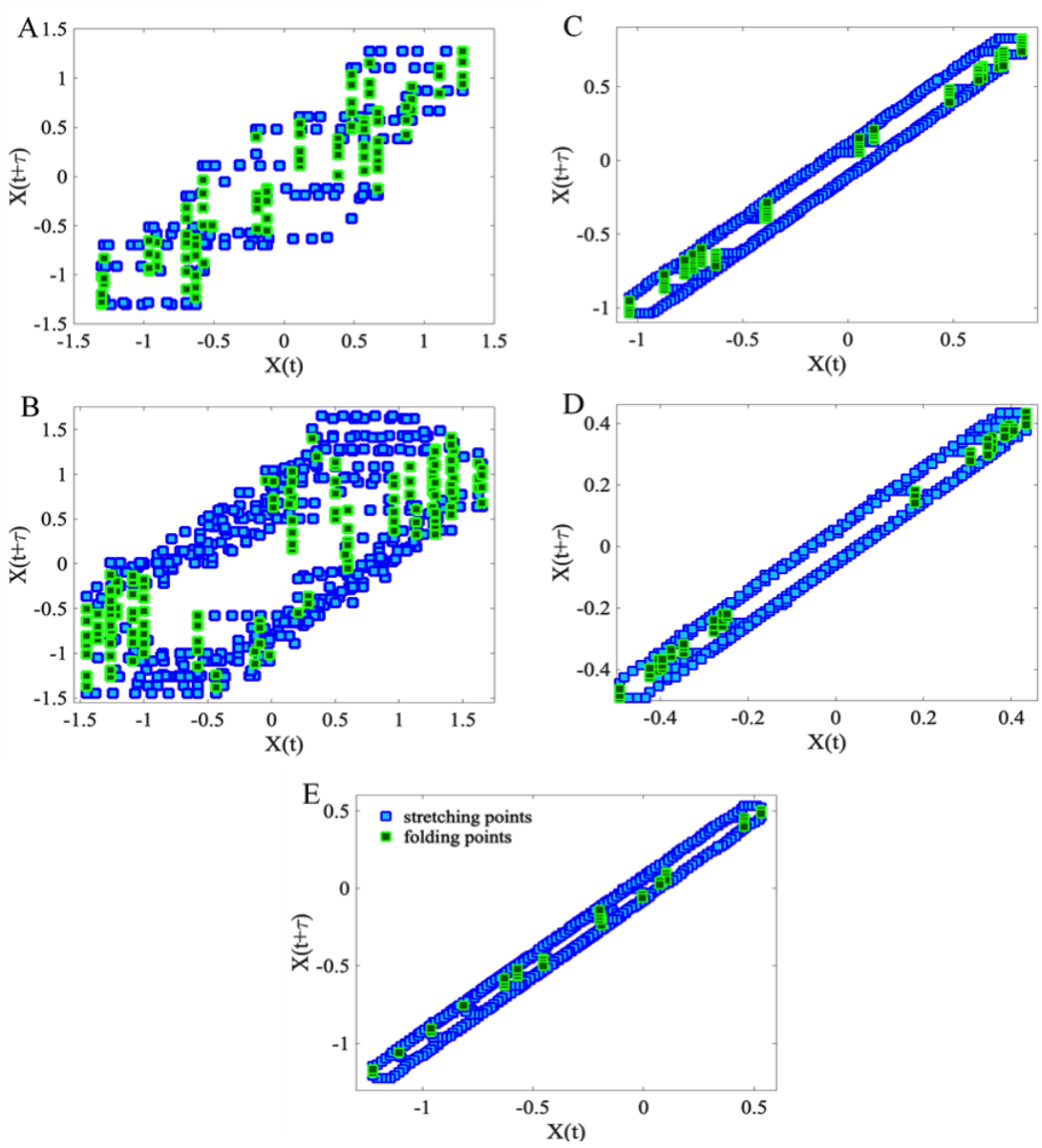

Fig. 7.

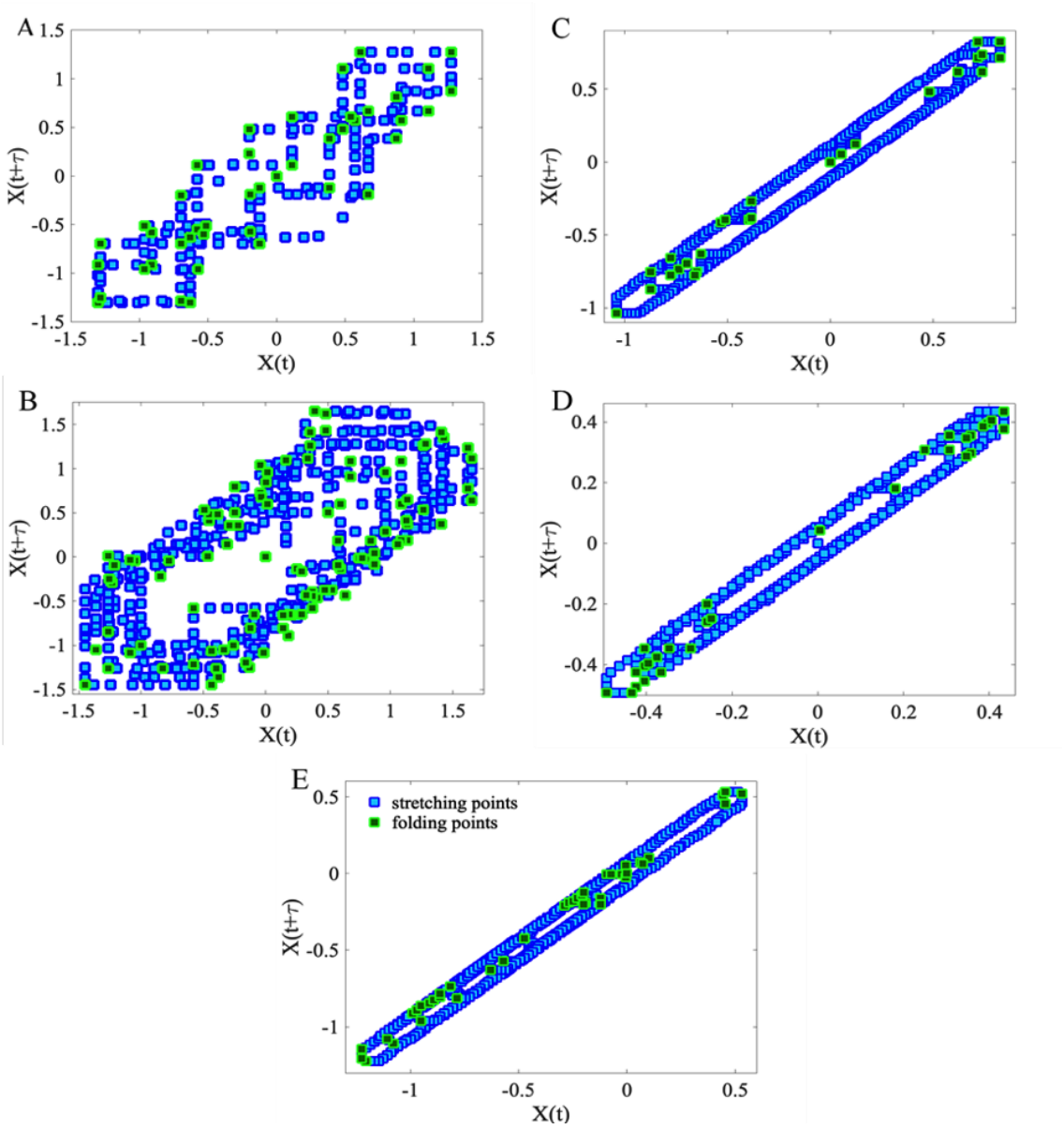

Fig. 8.

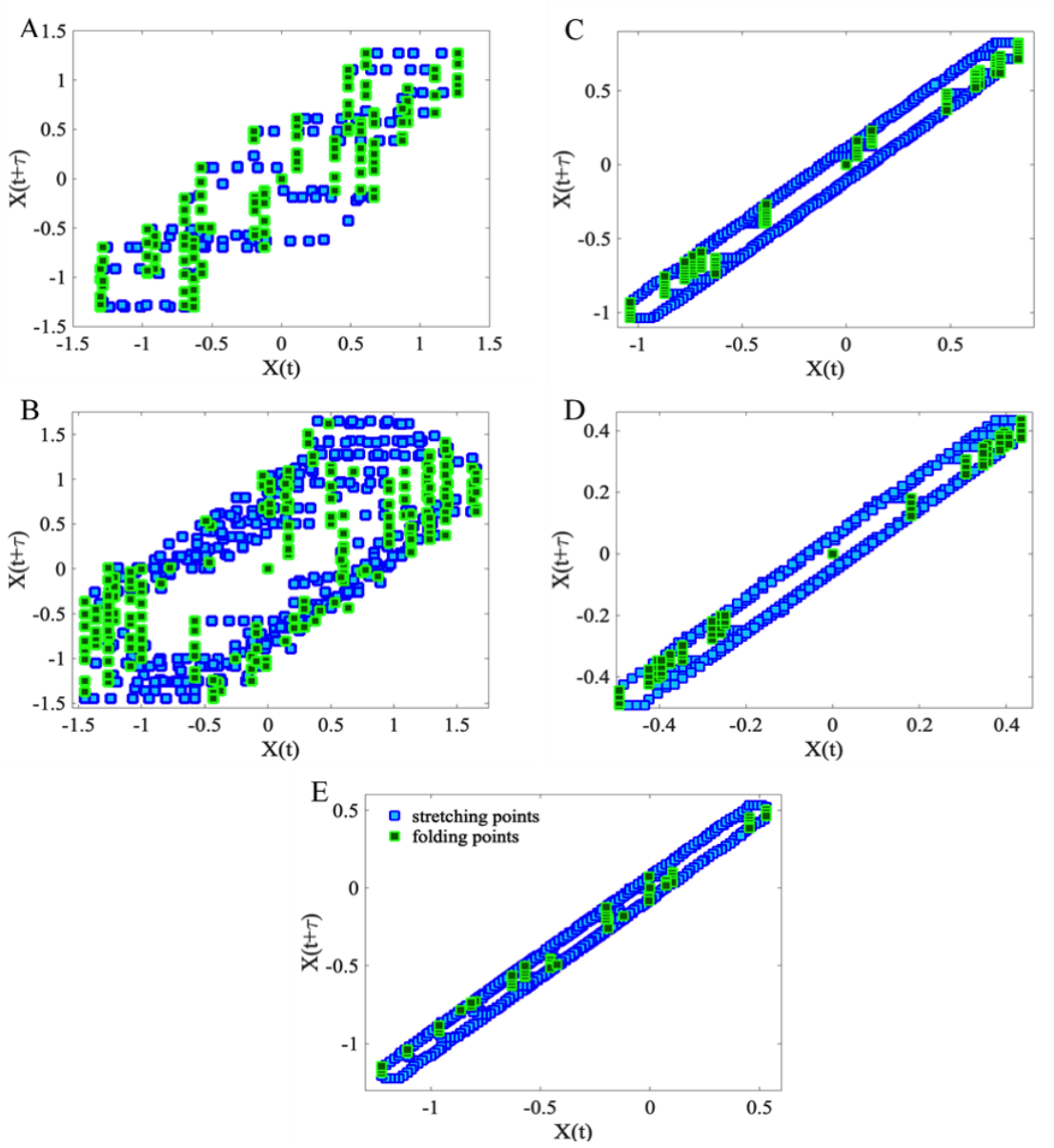

Fig. 9.

Table 1.

Tracking condition (frequency Hz)	**CD**	**FD**	**LLE**
Sinusoid (0.1 Hz)	1.0365 ± 0.118	1.2520 ± 0.0507	0.0182 ± 0.0068
Sinusoid (0.3 Hz)	1.2217 ± 0.0251	1.6773 ± 0.03	0.0230 ± 0.0012
Trapezoid (0.1 Hz)	1.0616 ± 0.0125	0.9784 ± 0.0338	0.0284 ± 0.0016
Trapezoid (0.3 Hz)	1.0673 ± 0.0151	1.7303 ± 0.0574	0.0308 ± 0.0012
Pseudo-periodic (0.117 Hz and 0.278 Hz)	1.0630 ± 0.009	1.7055 ± 0.0138	0.0533 ± 0.0047

Table 2.

Tracking condition (frequency Hz)	**CB method [34]**	**Modified CB method**	**Proposed method**
Sinusoid (0.1 Hz)	14.7634 ± 1.7141	62.1573 ± 4.5681	100
Sinusoid (0.3 Hz)	45.5992 ± 2.8285	85.2747 ± 3.0563	100
Trapezoid (0.1 Hz)	56.7946 ± 6.479	98.3128 ± 0.021	100
Trapezoid (0.3 Hz)	82.9169 ± 2.5869	99.89 ± 0.02	100
Pseudo-periodic (0.117 and 0.278 Hz)	80.49 ± 3.3431	99.9175 ± 0.0474	100

Fatemeh babazadeh received the B.S. and M.Sc. degrees in biomedical engineering in 2013 and 2015 from Shahed University, Tehran, Iran. Currently, she is a Ph.D. candidate in the biomedical engineering at Amirkabir University of Technology. Her research interests contain modeling, human motor control, neuromuscular control systems, nonlinear dynamics, and chaotic signals and systems.

Mohammad Ali Ahmadi-Pajouh received the B.S. in electrical engineering from K. N. Toosi University of Technology in 2003, the M.Sc. and Ph.D. degrees in biomedical engineering in 2007 and 2012 form Amirkabir University of Technology. His research interests are modeling, rehabilitation, human motor control, medical devices and robotics, and he has published several articles about mentioned issues in international journals and conferences. He is an Assistant Professor of biomedical engineering in Amirkabir University of Technology.

Seyyed Mohammad Reza Hashemi Golpayegani received the B.S. in electrical engineering from Amirkabir University of Technology, Tehran in 1968, the M.S. degree in electrical engineering from the University of Dayton in 1973, and the Ph.D. degree in biomedical engineering from the Ohio state University in 1976. He has published several books and articles in the fields of chaos, nonlinear dynamics and biomedical engineering. He is a Full Professor of biomedical engineering in Amirkabir University of Technology. His research interests are chaos, nonlinear dynamics, and complex systems.